Progress In Electromagnetics Research M, Vol. 93, 23–34, 2020

Low Sidelobe Cosecant-Squared Pattern Synthesis for Large Planar Array Using Genetic Algorithm

Tarek Sallam[1, 2, *] and Ahmed M. Attiya[3]

Abstract—A cosecant-squared radiation pattern synthesis for a planar antenna array by using the genetic algorithm (GA) is presented. GA makes array synthesis flexible to achieve two desired features, namely, low peak side lobe level (PSLL) and small deviation (ripples) in the shaped beam region. In order to obtain a desired $\csc^2$ pattern with the PSLL constrained, GA optimizes both the excitation amplitude and phase weights of the array elements. Dynamic range ratio (DRR) of the excitation amplitudes is improved by eliminating the weakly excited array elements from the optimized array without distorting the obtained pattern. To illustrate the effectiveness and advantages of GA, the beam pattern with specified characteristics is obtained for the same array by using particle swarm optimization (PSO). Results show that the performances of GA and PSO are comparable when dealing with small-to-moderate planar antenna arrays. However, GA significantly outperforms PSO on large arrays. Moreover, numerical results reveal that GA is superior to PSO in terms of cost function evaluation and statistical tests.

1. INTRODUCTION

Antenna arrays with a cosecant-square shaped beam pattern are most often employed by airborne search radars to observe ground targets, as well as by ground-based radars to detect aircraft targets [1]. Coverage of a simple fan beam is usually inadequate for targets at high altitudes close to the radar [2]. A simple fan-beam antenna radiates very little of its energy in this direction. However, there are a few techniques for modifying the antenna pattern to radiate more energy at higher angles. One technique for accomplishing this is to employ a beam with a shape proportional to the square of the cosecant of the elevation angle [2]. Moreover, a cosecant-squared antenna produces a constant echo-signal power, independent of the target range, for a target flying at a constant altitude.

Many advanced shaped pattern synthesis methods were presented like analytical techniques [3, 4], iterative sampling method [5], alternating projection method [6, 7], mathematical programming-based optimization techniques [8, 9], and deterministic methods [10]. Owing to the complexity of the shaped pattern synthesis, most of synthesis methods can be considered as stochastic optimization algorithms, such as particle swarm optimization (PSO) [11, 12], differential evolution algorithm [13], firefly algorithm [14], simulated annealing [15], tabu search algorithm [16], ant colony optimization [17], and gravitational search algorithm (GSA) [18].

Modern communication, imaging, and sensing systems require using large antenna arrays to offer better capacity, higher resolution, and improved sensitivity. Examples of large array systems include massive MIMO systems [19], weather radar [20], satellite communication [21], as well as the next generation of radio telescopes [22].

Received 20 April 2020, Accepted 14 May 2020, Scheduled 27 May 2020

* Corresponding author: Tarek Sallam (tarek.sallam@feng.bu.edu.eg).

[1] Faculty of Electronic and Information Engineering, Huaiyin Institute of Technology, Huai'an, Jiangsu 223002, China. [2] Faculty of Engineering at Shoubra, Benha University, Cairo, Egypt. [3] Microwave Engineering Department, Electronics Research Institute (ERI), Cairo, Egypt.

Synthesizing shaped power patterns is a highly nonlinear problem especially when dealing with large arrays due to the increase of the dimensionality of the problem, and hence its complexity. Stochastic optimization algorithms would be good choices in dealing with this problem because of their powerful search schemes to find the global optimum. Among them, Genetic algorithm (GA) is one demonstrating powerful global optimizer [23, 24]. GA is an excellent stochastic global optimization approach which is part of a larger field of evolutionary computations. This approach models genetics and natural selection in order to optimize a given cost function [27, 28]. Since its introduction, the GA has become a dominant numerical optimization algorithm in many disciplines. Details on implementing a GA can be found in [29], and a variety of applications to electromagnetics are reported in [23]. Some of the advantages of the GA include: (a) optimizing continuous or discrete variables, (b) avoiding calculation of derivatives, (c) handling a large number of variables, (d) suitability for parallel computing, (e) jumping out of a local minimum, (f) providing a list of optimum variables, not just a single solution, and (g) working with numerically generated data, experimental data, or analytical functions.

In this paper, GA is chosen to optimize both the element excitation amplitude and phase weights (complex excitation weights) for obtaining a cosecant-squared pattern with constrained peak sidelobe level (PSLL). The goal is to optimize these weights to attain the desired performance, which is basically a pattern with low ripples in the cosecant-squared region and low PSLL.

In order to examine the effectiveness of GA in shaping the beam pattern, it is compared to PSO on two planar arrays of different array sizes. The first one, representing a small-to-moderate array, is a 16×16-element array. The second one is a 32×32-element array which represents a large planar array. The numerical results show that for the 16×16-element array, GA and PSO are competitive, while for the 32×32-element array, the GA is highly superior to the PSO in terms of both the deviation in the $\csc^2$ shaped region and the obtained PSLL. Furthermore, to verify the superiority of GA, various quality metrics have been taken into consideration such as cost function evaluation and convergence as well as the Wilcoxon's rank sum test [25] as a statistical test.

2. $\mathbf{Csc^2}$ PATTERN SYNTHESIS FORMULATION

The array factor $AF(\theta, \phi)$ of a rectangular planar antenna array, having $M \times N$ isotropic elements arranged along a rectangular grid and spaced by d_x in the x-direction and d_y by in the y-direction, can be written as [26]

$$AF\left(\theta, \phi\right) = \sum_{m=0}^{M-1} \sum_{n=0}^{N-1} A_{mn} e^{jk(md_x u + nd_y v)} \tag{1}$$

where A_{mn} is the complex excitation weight of the (m, n)th element, k the free space wavenumber $(2\pi/\lambda)$, λ the wavelength, $u = \sin\theta\cos\phi$, and $v = \sin\theta\sin\phi$.

Figure 1 shows the cosecant-squared pattern mask function representing the desired pattern shape at a specific ϕ. The $\csc^2$ shaped region has an angular span of $\theta_{\min} \leq \theta \leq \theta_{\max}$. The desired PSLL (defined as -30 dB as shown in Fig. 1) is required over $-90^{\circ} \leq \theta \leq \theta_{\rm o}$ and $\theta_{\max} < \theta \leq 90^{\circ}$. The region $\theta_{\rm o} < \theta < \theta_{\min}$ is assumed to be a transition region. Accordingly, the $\csc^2$ mask function at a given ϕ is defined in dB as follows

$$Mask\left(\theta\right) = \begin{cases} 10\log_{10}\left(\dfrac{\csc^2\theta}{\csc^2\theta_{\min}}\right), & \theta_{\min} \leq \theta \leq \theta_{\max} \\ Desired\ PSLL, & -90^{\circ} \leq \theta \leq \theta_{\rm o}, \quad \theta_{\max} \leq \theta \leq 90^{\circ} \\ 0, & \theta_{\rm o} \leq \theta \leq \theta_{\min} \end{cases} \tag{2}$$

To achieve the cosecant-squared radiation pattern, the array excitation weights should be determined through an optimization (minimization) of a properly defined cost function that covers the concerns of the designer. Referring to Fig. 1, the radiation pattern must fit the ideal cosecant-squared radiation pattern *Mask* in the angular span $\theta_{\min} \leq \theta \leq \theta_{\max}$. Furthermore, the radiation pattern must be kept below the desired PSLL outside this angular region. The radiation pattern is normalized to its maximum value at $\theta_{\min}$. By sampling the AF in Eq. (1) and *Mask* in Eq. (2) at q points, the cost function, at a certain ϕ, is defined in dB as

$$Cost = \frac{1}{q}(w_1\Delta_{\rm SLL} + w_2\Delta_{\csc^2}) \tag{3}$$

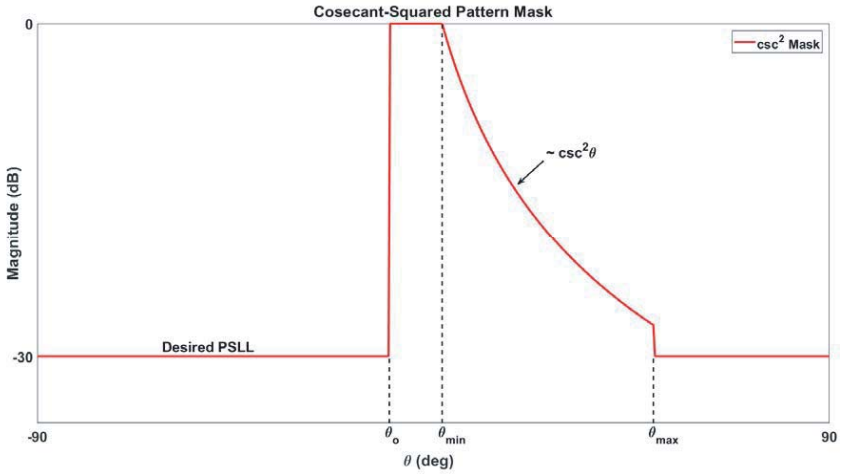

Figure 1. The cosecant-squared pattern mask showing the $\csc^2$ shaped region and a desired PSLL of -30 dB.

where w_1 and w_2 are weighting factors for the SLL and the $\csc^2$ pattern Mask in the required angular span. The Δ_{SLL} is based on "Don't Exceed" error criterion function as follows

$$\Delta_{\text{SLL}} = \sum_{\theta=-90^\circ}^{\theta_o} \varepsilon(\theta) + \sum_{\theta=\theta_{\text{MAX}}}^{+90^\circ} \varepsilon(\theta) \tag{4a}$$

The "Don't Exceed" error criterion of the PSLL is given by

$$\varepsilon(\theta) = \frac{1 + \text{sgn}(AF(\theta) - Mask(\theta))}{2} [AF(\theta) - Mask(\theta)] \tag{4b}$$

On the other hand, the cost of the error due to the deviation (ripples) in the $\csc^2$ shaped region is given by

$$\Delta_{\csc^2} = \sum_{\theta=\theta_{\min}}^{\theta_{\max}} |AF(\theta) - Mask(\theta)| \tag{5}$$

Apparently, the smaller the cost value is, the more fit the array distribution is and the better the match is between the obtained pattern and the desired one. An optimal solution is defined as a solution which does not violate the mask which results in a minimum or zero cost function.

3. ALGORITHM OVERVIEW AND PARAMETRIC SETUP

3.1. Overview of Genetic Algorithm

The GA implemented here is simple and flexible for pattern synthesis of arbitrary arrays. This approach avoids binary coding and directly deals with real or complex weighting vectors. Using this approach, constraints on the phases and magnitudes of the complex weights are easily imposed for practical implementation of phase shifters and attenuators.

The GA begins with a random set of array configurations called the *population* (rows of a matrix for linear array and matrices of a tensor in the case of planar array) consisting of variables of each array element amplitude/phase. Each array configuration is evaluated by the cost function that returns a numerical value or score that characterizes how well the array configuration performs. Array configurations with high costs are discarded, while array configurations with low costs form a mating pool. Two parents are randomly selected from the mating pool. Selection is inversely proportional to the cost. Offspring result from a combination of the parents. The offspring replace the discarded array configurations. Next, random array configurations in the population are randomly modified or

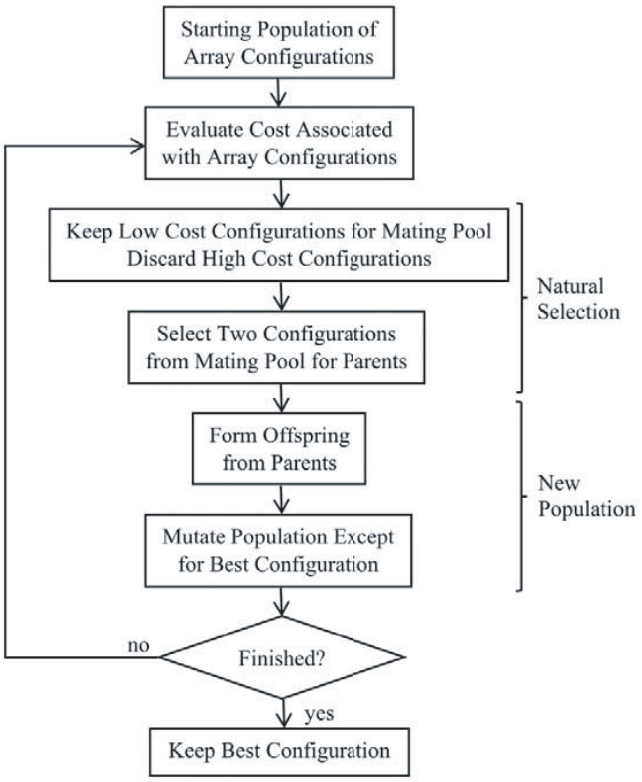

Figure 2. Flowchart of the GA.

mutated. Finally, the new array configurations are evaluated for their costs, and the process repeats. The flowchart of the GA appears in Fig. 2.

In this paper, the array is planar, and hence each array configuration is a matrix (called *chromosome*) containing the number of columns equal to the number of elements in y direction N, and the number of rows equals the double of the number of elements in x direction M (the upper half for amplitude and lower half for phase). In this way and without any array symmetry assumptions, the chromosome is a $2M \times N$ matrix.

3.2. Details of Parametric Setup

From the above discussion, the individuals of population (to be optimized) of GA and PSO are $2M \times N$ matrices. The top $M \times N$ matrix contains real-valued numbers ranging from 0 to 1 which represent the excitation amplitudes, and the bottom $M \times N$ matrix also contains real-valued numbers ranging from $-\pi$ to π which represent the excitation phases.

Based on the guidelines provided in [30], two-point crossover is chosen for GA. Mutation probability is taken as 0.04, and "Roulette Wheel" Selection is considered for the presented problem. For PSO, the values of learning factors c_1 and c_2 are chosen as 2. The inertia weight and maximum allowable velocity are held fixed throughout the optimization process at 0.4 and 0.3, respectively [30]. For both algorithms, the population size is taken as 10, and the termination condition is chosen as a maximum iteration of 1000.

4. NUMERICAL RESULTS

With reference to Fig. 1, the values $\theta_o = 0°$, $\theta_{\min} = 6°$, $\theta_{\max} = 30°$, and desired PSLL $= -30\,\text{dB}$ are considered for the optimization procedure. This ensures a $\csc^2$ shaped beam of angular width 30°. Extending this angular width and/or realizing lower PSLL only increase the computational burden, but

the optimization procedure remains the same. Realizing the cosecant-squared beam is usually more important and computationally intensive than reducing the PSLL. As a result, the weighting factors of the cost function are selected as $w_1 = 0.1$ and $w_2 = 0.9$.

A far-field pattern of $q = 1000$ points evenly spaced in sine space is computed for each candidate array at each cost evaluation, which provides a good sampling of the far-field pattern. Two different size square arrays of isotropic elements with a square grid of inter-element spacing $d_x = d_y = 0.5\lambda$ are considered. The results presented in this section are the best set of results obtained from 50 independent runs of each of the algorithms for each array size. Meanwhile, in the tabulated results, the best result between GA and PSO is highlighted in **boldface**. All results are presented at $\phi = 0°$.

4.1. Small-to-Moderate Planar Arrays

A 16×16-element array is taken as an example of small-to-moderate planar arrays. In this case, each chromosome (or a particle for PSO) is $(2 \times 16) \times 16 = 32 \times 16$ matrix. Hence, the total dimension of the optimization problem is 512. Fig. 3 shows the optimized $\csc^2$ patterns using GA and PSO for the 16×16-element array along with the $\csc^2$ mask. It can be seen that PSO is competitive with GA w.r.t obtained PSLL and ripples in the mainbeam ($\Delta_{\csc^2}$). For both algorithms, the deviation in the $\csc^2$ shaped beam is much less than the deviation in PSLL. Both algorithms have very low mainbeam ripple, while most of deviation of PSLL concentrates in the near-in sidelobes. The design (desired) specification of PSLL and $\Delta_{\csc^2}$ and their corresponding obtained values are shown in the upper half of Table 1. It can be noticed that GA has a little bit better values of PSLL and $\Delta_{\csc^2}$ than those of PSO. The optimum excitation amplitude and phase weights of the array elements from GA are shown in Fig. 4. The convergence characteristics of the two algorithms are shown in Fig. 5. As can be seen, the convergence of GA is better and faster than PSO in terms of minimizing the cost function of Eq. (3).

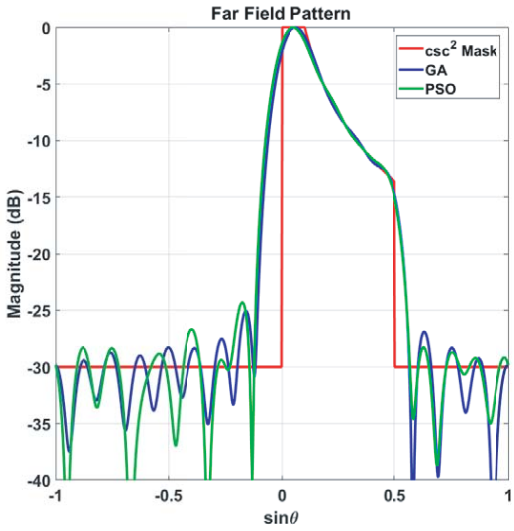

Figure 3. Optimized $\csc^2$ patterns for the 16×16-element array.

4.2. Large Planar Arrays

A 32×32-element array is taken as an example for large planar arrays. In this case, each chromosome or a particle is a $(2 \times 32) \times 32 = 64 \times 32$ matrix. Hence, the total dimension of the optimization problem is 2048 (four times that of 16×16 array). Fig. 6 shows the optimized $\csc^2$ patterns using GA and PSO for the 32×32-element array along with the $\csc^2$ mask. As shown, the PSO in this case performs very badly and cannot handle the beam-shaping problem anymore. This may be because the PSO algorithm is too simple to tackle the current optimization problem particularly when its dimension, and hence its complexity, becomes four times the previous one. For GA, as can be seen from Fig. 6, the deviation

Table 1. Desired and obtained results for the 16 × 16-element array.

Parameter	Desired	GA	PSO
PSLL (dB)	–30.00	**–25.04**	–24.30
$\Delta_{\csc^2}$ (dB)	0.00	**0.05**	0.13
DRR	—	149.81	42.55
After removing the weakly excited elements from the array			
PSLL (dB)	–30.00	–24.86	**–25.06**
$\Delta_{\csc^2}$ (dB)	0.00	**0.05**	0.16
DRR	—	8.68	7.41
# of removed elements	—	29	49

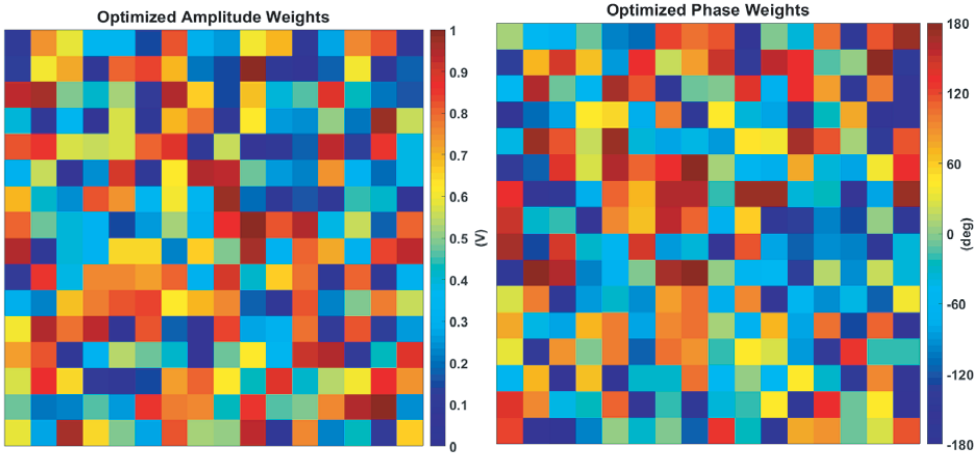

Figure 4. Optimized element excitation weights from the GA for the 16 × 16-element array (each square represents an element). (a) Amplitude. (b) Phase.

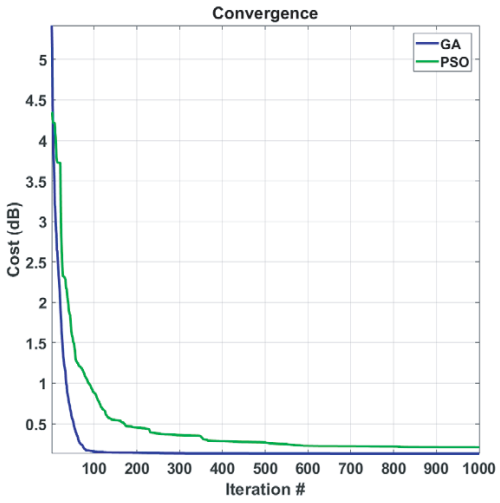

Figure 5. Convergence curves for the 16 × 16-element array.

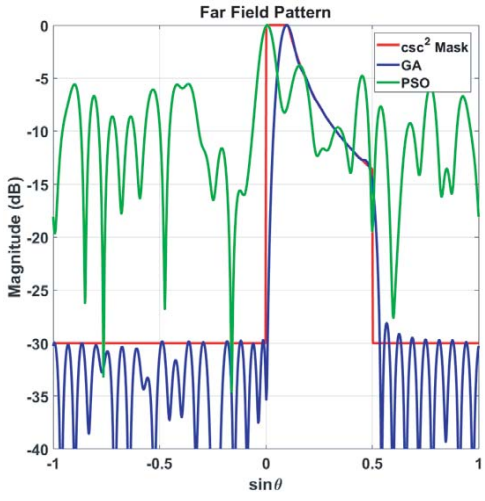

Figure 6. Optimized $\csc^2$ patterns for the 32×32-element array.

in PSLL becomes less (better PSLL) than that of 16×16 array in Fig. 3, while its performance in the $\csc^2$ shaped region nearly remains unchanged (both arrays have almost zero ripples in the shaped mainbeam). The first near-in sidelobe on the right of the mainbeam in Fig. 6 has most of the deviation over desired PSLL then the next one to it. The upper half of Table 2 shows the desired and obtained values of PSLL and $\Delta_{\csc^2}$ for the 32×32 array. From Table 2, it can be noted that PSO is in this case very far from being competitive with GA in terms of $\csc^2$ shaped beam and achieved PSLL. The optimized excitation amplitude and phase weights of the array elements from GA are shown in Fig. 7. The convergence curves of the cost function are presented in Fig. 8. In this case PSO has a lack of convergence, while the convergence performance of GA is consistent with its counterpart in 16×16 array.

Table 2. Desired and obtained results for the 32×32-element array.

Parameter	**Desired**	**GA**	**PSO**
PSLL (dB)	–30.00	**–28.12**	–5.54
$\Delta_{\csc^2}$ (dB)	0.00	**0.03**	13.67
DRR	—	2846.60	14.77
After removing the weakly excited elements from the array			
PSLL (dB)	–30.00	**–27.56**	–5.47
$\Delta_{\csc^2}$ (dB)	0.00	**0.05**	14.00
DRR	—	9.72	9.43
# of removed elements	—	112	77

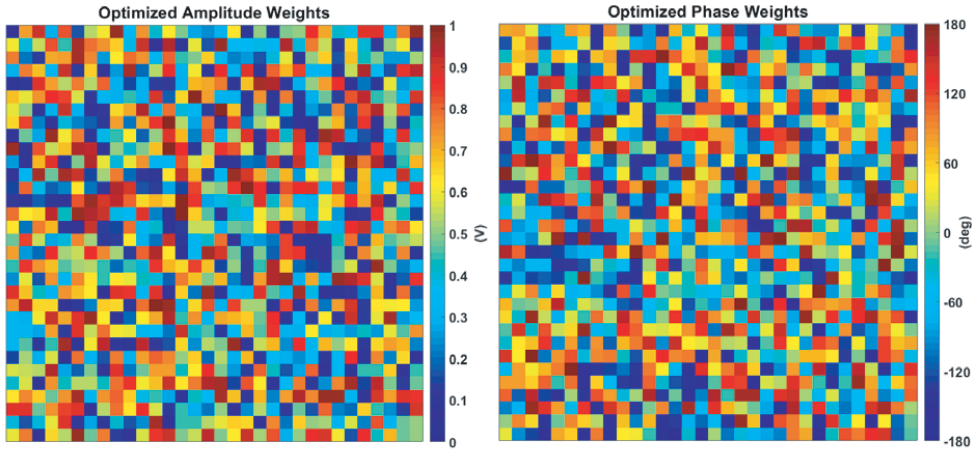

(a) (b)

Figure 7. Optimized element excitation weights from the GA for the 32×32-element array. (a) Amplitude. (b) Phase.

4.3. DRR Improvement

The dynamic range ratio (DRR) controls the maximum-to-minimum excitation amplitude ratio, i.e.,

$$DRR = \frac{|A_{mn}|_{\max}}{|A_{mn}|_{\min}} \tag{6}$$

whose reduction leads to a simplification of the feed network and to an increase of the illumination efficiency [31]. Usually, the excitation amplitudes are normalized to its maximum, so $|A_{mn}|_{\max}$ is 1. To

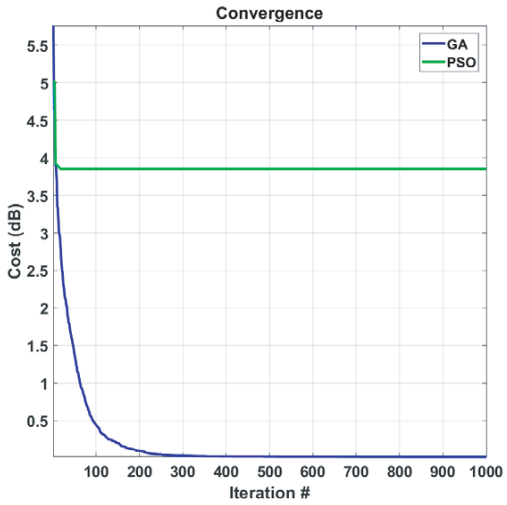

Figure 8. Convergence curves for the 32 × 32-element array.

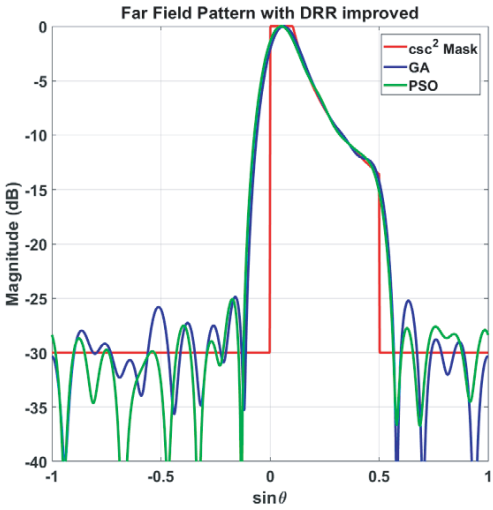

Figure 9. Optimized $\csc^2$ patterns for the 16×16-element array after removing the weakly excited elements from the array.

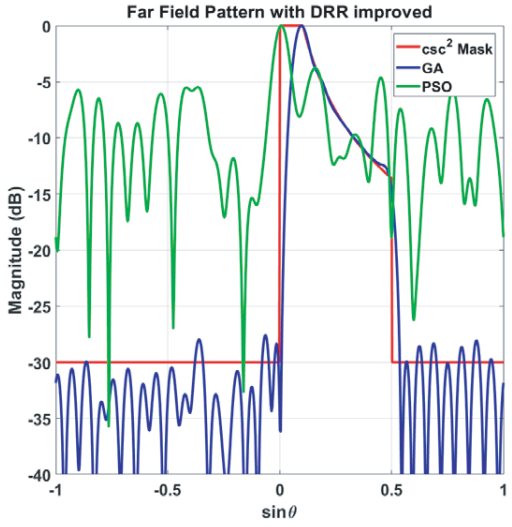

Figure 10. Optimized $\csc^2$ patterns for the 32 × 32-element array after removing the weakly excited elements from the array.

keep the dynamic range ratio within a tolerable range (1–10), the elements having normalized amplitudes below 0.1 are assumed to be passively terminated with matched loads or open circuited for each of the two arrays with minor change in the beam pattern.

The obtained beam patterns for the 16 × 16 and 32 × 32 arrays, after removing the weakly excited elements from the optimized array, are shown in Figs. 9 and 10, respectively, which clearly reflect negligible changes in comparison with Figs. 3 and 6, respectively. Fig. 11 shows the optimized element excitation amplitude weights from the GA after removing the weakly excited elements for the two arrays. The upper halves of Tables 1 and 2 show the DRR before improvement for the 16 × 16 and 32 × 32 arrays, respectively, while their lower halves show the DRR after improvement, i.e., after removing the weakly excited elements from the optimized array. Also, the lower halves of the two tables show the values of design parameters (PSLL and $\Delta_{\csc^2}$), along with the number of removed elements, after DRR improvement. From Tables 1 and 2, it is obvious that the reduction in GA's DRR is much bigger than

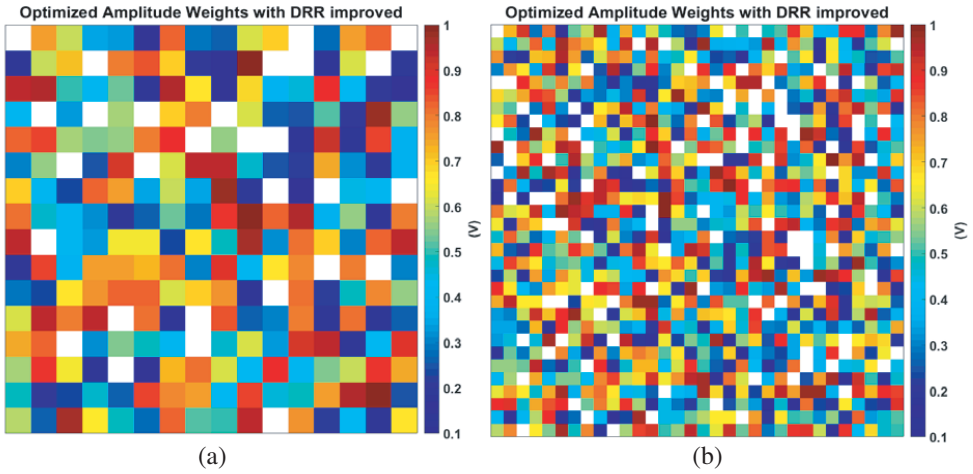

Figure 11. Optimized element excitation amplitude weights from the GA after removing the weakly excited elements from the array (white squares). (a) 16×16-element array. (b) 32×32-element array.

that of PSO's DDR. Moreover, it can be seen that while there are small changes in the values of design parameters before and after DRR improvement, the DRR itself is greatly reduced (for 32×32 array using GA, its value is reduced from 2846.60 to 9.72!).

4.4. Statistical Analysis and Computational Time

The best, worst, mean, and standard deviation (STD) values of the cost function of GA and PSO over 50 independent runs are recorded and compared for each array in Table 3. As can be seen in Table 3, the GA can expose excellent results in all problem dimensions (different array sizes), and its performance remains consistently superior when realizing cases with many variables (high dimension as in large array). It is also observed that the optimality of results and the performance of PSO are significantly degraded by increasing the dimension of the problem when dealing with large arrays.

Table 3. Cost function values over 50 runs.

Array	Metric	GA	PSO
16×16	Best	**0.13**	0.21
	Worst	**1.09**	5.29
	Mean	**0.54**	2.58
	STD	**0.36**	1.60
32×32	Best	**0.02**	3.85
	Worst	**0.66**	6.79
	Mean	**0.28**	5.56
	STD	**0.19**	0.66

Furthermore, Wilcoxon's rank sum test [25] is used to examine whether the performance of the GA is significantly better than PSO in this work. In the Wilcoxon's rank sum test, if the p-value achieved is less than 0.05 (5% significance level), then the performances of the two algorithms are significantly different; otherwise, the performances of the two algorithms are similar. Table 4 shows the p-values obtained through Wilcoxon's rank sum test between GA and PSO for the two different sizes of array. All the p-values are less than 0.05, which is a strong proof against the null hypothesis indicating that the attained results by the best algorithm, GA, versus PSO are statistically significant and have not

Table 4. *P*-values of Wilcoxon's rank sum test of GA versus PSO.

Array	*P*-Value
16×16	2.44E-11
32×32	7.07E-18

occurred by chance.

The average computational time over the 50 runs taken by the two algorithms for the two arrays can be found in Table 5. Obviously, the PSO algorithm is the fastest, although it cannot give the best results especially for the large array. It is worth noting that evaluating a meta-heuristic algorithm should be comprehensive and objective, not just from a single aspect. The GA presents better results in terms of cost function evaluation and convergence, despite not the fastest. Thus, GA can be considered as an efficient technique for the $\csc^2$ pattern synthesis.

Table 5. The average computational time (in seconds) over the 50 runs.

Array	GA	PSO
16×16	49.58	**12.22**
32×32	85.49	**14.19**

5. CONCLUSION

Synthesis of a cosecant-square shaped beam pattern with low PSLL from a planar array antenna using GA has been proposed and assessed by comparing its performance to that of PSO. For the synthesis of the shaped beam pattern, the desired PSLL ($-30\,\text{dB}$) and the $\csc^2$ mainbeam ripple are simultaneously taken into account by minimizing properly formulated cost function using GA and PSO. The desired shaped beams for two different array sizes, namely, small-to-moderate and large planar arrays, are achieved using the two optimization algorithms. For the small-to-moderate planar array, it has been shown that PSO is competitive with GA. However, GA has been found to be remarkably superior to PSO for the large planar array. The numerical results show that the GA can achieve a low PSLL (about $-25\,\text{dB}$ for small-to-moderate array and $-28\,\text{dB}$ for large array) and a $\csc^2$ mainbeam with almost zero ripple for either array. This reflects the effectiveness of the GA for generating $\csc^2$ shaped beams.

The presented method incorporates turning-off of the weakly excited array elements from the optimized array, which greatly reduces the DRR of the array, especially for GA, with a negligible change in the resultant beam pattern. Reducing the DDR of the array is helpful for reliable design of the feed network.

The comparative performance of GA and PSO clearly shows the superiority of GA over PSO in terms of finding optimum solutions (i.e., best final cost function values) for the presented problem. The quality of the solutions produced individually using GA and PSO is analyzed statistically using the Wilcoxon's rank sum test, and the meaningful advantages of GA over PSO are proven for the proposed problem. To sum up, GA is a powerful tool to solve the low sidelobe cosecant-squared pattern synthesis problem especially for large planar arrays. The presented method can also be extended for generating other shaped beams for different array configurations.

REFERENCES

1. Elliott, R. S., *Antenna Theory and Design*, Wiley, New York, NY, USA, 2003.
2. Skolnik, M., *Introduction to Radar Systems*, McGraw-Hill, Tokyo, 1981.

3. Woodward, P. M. and J. D. Lawson, "The theoretical precision with which an arbitrary radiation pattern may be obtained from a source of a finite size," *J. IEE*, Vol. 95, No. 37, 363–370, Sep. 1948.
4. Li, J.-Y., Y.-X. Qi, and S.-G. Zhou, "Shaped beam synthesis based on superposition principle and Taylor method," *IEEE Trans. Antennas Propag.*, Vol. 65, No. 11, 6157–6160, Nov. 2017.
5. Stutzman, W., "Synthesis of shaped-beam radiation patterns using the iterative sampling method," *IEEE Trans. Antennas Propag.*, Vol. 19, No. 1, 36–41, Jan. 1971.
6. Quijano, J. L. A. and G. Vecchi, "Alternating adaptive projections in antenna synthesis," *IEEE Trans. Antennas Propag.*, Vol. 58, No. 3, 727–737, Mar. 2010.
7. Haddadi, A., A. Ghorbani, and J. Rashed-Mohassel, "Cosecant-squared pattern synthesis using a weighted alternating reverse projection method," *IET Microw., Antennas Propag.*, Vol. 5, No. 15, 1789–1795, 2011.
8. Fuchs, B., A. Skrivervik, and J. R. Mosig, "Shaped beam synthesis of arrays via sequential convex optimizations," *IEEE Antennas Wireless Propag. Lett.*, Vol. 12, 1049–1052, 2013.
9. Echeveste, J. I., M. A. G. de Aza, and J. Zapata, "Shaped beam synthesis of real antenna arrays via finite-element method, floquet modal analysis, and convex programming," *IEEE Trans. Antennas Propag.*, Vol. 64, No. 4, 1279–1286, Apr. 2016.
10. Bucci, O. M., T. Isernia, and A. F. Morabito, "An effective deterministic procedure for the synthesis of shaped beams by means of uniformamplitude linear sparse arrays," *IEEE Trans. Antennas Propag.*, Vol. 61, No. 1, 169–175, Jan. 2013.
11. Pirhadi, A., M. H. Rahmani, and A. Mallahzadeh, "Shaped beam array synthesis using particle swarm optimisation method with mutual coupling compensation and wideband feeding network," *IET Microw., Antennas Propag.*, Vol. 8, No. 8, 549–555, Jun. 2014.
12. Abo El-Hassan, M., K. H. Awadalla, and K. F. Hussein, "Shaped-beam circularly polarized antenna array of linear elements for satellite and SAR applications," *Wireless Pers. Commun.*, Vol. 110, 605–619, 2020.
13. Yang, X., L. Chang, J. Zhang, D. Li, and M. Zhang, "A cosecant squared beam antenna array operating at 5.85–7.6 GHz," *2019 Cross Strait Quad-Regional Radio Science and Wireless Technology Conference (CSQRWC)*, 1–3, Taiyuan, China, 2019.
14. Krishna Chaitanya, R., G. S. N. Raju, K. V. S. N. Raju, and P. Mallikarjuna Rao, "Antenna pattern synthesis using the quasi Newton method, firefly and particle swarm optimization techniques," *IETE Journal of Research*, 1–9, 2019.
15. Ferreira, J. A. and F. Ares, "Pattern synthesis of conformal arrays by the simulated annealing technique," *Electron. Lett.*, Vol. 33, No. 14, 1187–1189, Jul. 1997.
16. Ho, S. L. and S. Yang, "Multiobjective synthesis of antenna arrays using a vector tabu search algorithm," *IEEE Antennas Wirel. Propag. Lett.*, Vol. 8, 947–950, Aug. 2009.
17. Akdagli, A. A., K. Guney, and D. Karaboga, "Touring ant colony optimization algorithm for shaped-beam pattern synthesis of linear antenna," *Electromagnetics*, Vol. 26, 615–628, 2006.
18. Chatterjee, A., G. K. Mahanti, and P. R. S. Mahapatra, "Design of fully digital controlled reconfigurable dual-beam concentric ring array antenna using gravitational search algorithm," *Progress In Electromagnetics Research C*, Vol. 18, 59–72, 2011.
19. Larsson, E. G., O. Edfors, F. Tufvesson, and T. L. Marzetta, "Massive MIMO for next generation wireless systems," *IEEE Commun. Mag.*, Vol. 52, No. 2, 186–195, Feb. 2014.
20. Vollbracht, D., "System specification for dual polarized low power X-band weather radars using phased array technology," *Proc. Int. Radar Conf.*, 1–6, Lille, France, Oct. 2014.
21. Sallam, T. and A. M. Attiya, "Different array synthesis techniques for planar antenna array," *Applied Computational Electromagnetics Society Journal*, Vol. 34, No. 5, 716–723, 2019
22. Bregman, J. D., "Concept design for a low-frequency array," *Proc. SPIE*, Vol. 4015, 19–33, Jul. 2000.
23. Haupt, R. and D. Werner, *Genetic Algorithms in Electromagnetics*, 1st edition, Wiley-IEEE Press, 2007.

24. You, P., Y. Liu, K. D. Xu, C. Zhu, and Q. H. Liu, "Generalisation of genetic algorithm and fast Fourier transform for synthesising unequally spaced linear array shaped pattern including coupling effects," *IET Microw., Antennas Propag.*, Vol. 11, No. 6, 827–832, May 2017.
25. Derrac, J., S. García, D. Molina, and F. Herrera, "A practical tutorial on the use of nonparametric statistical tests as a methodology for comparing evolutionary and swarm intelligence algorithms," *Swarm EVol. Comput*, Vol. 1, 3–18, 2011.
26. Balanis, C. A., *Antenna Theory: Analysis and Design*, 4th edition, John Wiley & Sons, Inc, New York, 2016.
27. Holland, J. H., "Genetic algorithms," *Scientific American*, 66–72, Jul. 1992.
28. Goldberg, D. E., *Genetic Algorithms in Search, Optimization, and Machine Learning*, Addison-Wesley, Reading, MA, 1989.
29. Haupt, R. L. and S. E. Haupt, *Practical Genetic Algorithms*, 2nd edition, John Wiley & Sons, New York, 2004.
30. Boeringer, D. W. and D. H. Werner, "Particle swarm optimization versus genetic algorithms for phased array synthesis," *IEEE Trans. Antennas Propag.*, Vol. 52, No. 3, 771–779, Mar. 2004.
31. Morabito, A. F., A. Massa, P. Rocca, et al., "An effective approach to the synthesis of phase-only reconfigurable linear arrays," *IEEE Trans. Antennas Propag.*, Vol. 60, No. 8, 3622–3631, 2012.